ChemTech

Preparation of TiO₂ Nanotube Arrays Electrode for Photoelectrochemical Water Splitting: Effect of Anodization Potential on Morphology and Photocurrent Response

Hedi Surahman*, Yuni K Krisnandi and Jarnuzi Gunlazuardi

Departement of Chemistry University of Indonesia, Kampus Baru Depok, 16424, Indonesia

Abstract : In this work, highly ordered TiO₂ nanotubes arrays electrode were prepared by anodic oxidation of titanium foil under different anodization potentials in ethylene glycol electrolytes containing NH₄F and water. The morphology and photocurrent response of TiO₂ nanotubes arrays (TNTAs) were characterized by FESEM and electrochemical working station. The result indicated that anodization voltage significantly affects morphology structures and photoelectrocemical properties of TNTAs. The pore diameter, photocurrent response and water splitting photoconversion efficiency of TNTAs increased with anodization voltage.

Keywords: Anodization, Photocurrent, Photoelectrochemical, TiO₂ Nanotubes.

Introduction

In recent years, heterogeneous photo catalyst has attracted increasing attention in the field of sustainable and renewable energy such as photo electrochemical cell for hydrogen generation and photovoltaic cell for electricity generation[1-5]. A variety of semiconducting metal oxide has been use in this field[6-9]. Among them, TiO₂ is widely used as the photo catalyst electrode during the photo catalytic process, because it is chemical stability, low cost, nontoxicity and environment-friendly feature[10-13]. While there are still some shortcomings, including relatively low specific surface area and weak photo catalytic efficiency of bulk TiO₂ due to high recombination process of photogenerated electron and holes in the TiO₂ film. The nanostructures TiO₂, such as tubes, wires, dots, pillar, and fibers, have become a focus of considerable interest as they posses unique properties relevant to application in photo electrochemical cell. Among them, the material with tubular structure has been considered the most suitable way to achieve larger enhancement of surface area without an increase in the geometric area. The TiO₂ nanotubes also have more superior photocatalytic properties to be applied as photoelectrode because it has one-dimensional channels for charge transport so that the recombination of electrons and holes can be reduced. Several methods for the synthesis of TiO₂ nanotubes are electrochemical anodization[14-17], sol-gel[18], hydrothermal[19], template[20] and vapour deposition method[21]. The electrochemical anodization method using titanium foil in an electrolyte containg fluoride ions produce TNTAs with a packed structure and a uniform diameter and good mechanical properties and is suitable for photoelectrochemical water splitting applications.

The growth of TNTAs to several hundred nanometers have been reported first using anodizing method in fluoride acid solution[22]. Furthermore, the length of TNTAs to several hundred micrometers have been produced by anodization of titanium foil in organic electrolyte base containing fluoride ion[23]. The geometry parameters of TNTAs can be easily controlled by varying experimental conditions such as electrolyte

composition, anodization potential, anodization time and annealing temperature[24-27]. Some research on experiment condition of the TiO$_2$ nanotube arrays morphology have been reported[28-29]. Anodization potential play in important role on the TiO$_2$ nanotubes formation, which determines the pore diameter, wall thickness and tube length[30-31].

In this work, a series of TiO$_2$ nanotubes electrode were synthesized by electrochemical anodization of titanium foil in ethylene glycol electrolyte containing NH$_4$F and water under different anodization potentials for photoelectrochemical water splitting. The effect of anodization potential on the morphology structures, photocurrent response and photoconversion efficiency was systematically discussed.

Experimental

Preparation of TiO$_2$ nanotube arrays

Prior to the anodization, Ti foils (0,2 mm thick, 99,6% purity) were degreased at room temperature by sonicating in acetone and ethanol for 10 min, respectively, then rinsed with deionized water and dried in air. All anodization experiments were carried out in a two-electrode electrochemical cell at room temperature. Ti foils (4 cm x 1,5 cm x 0,02 cm) and stainless steel sheet (5 cm x 1,5 cm x 0,02 cm) were used as the anode and cathode, respectively. The distance between the two electrodes is kept at 1.5 cm in all the experiments. Ethylene glycol solution containing 0,3 wt% NH$_4$F and 2 vol% H$_2$O was used as electrolyte. The anodization process was performed with a direct current (DC) power supply for 30 min. The anodization voltage was varied from 15 V to 60 V in this study. After electrochemical treatment, the samples were rinsed with deionized water and dried in air. Then the obtained TNTAs were annealed at 450^{0}C for 2 h with a heating rate of 2^{0}C/min.

Material Characterization and Photoelectrochemical Measurements

The morphologies of the samples were observed using a field emission scanning electron microscope (FE-SEM, Inspect f50, FEI). Photoelectrochemical measurement were carried out in a three-electrode configuration with the as-prepared sample as the working electrode, Pt mesh as the counter electrode, and saturated Ag/AgCl as the reference electrode in 1 M KOH aqueous electrolyte. The photoelectrochemical cell consisting of a glass tube with a 2.5 cm diameter and height 5 cm is made of quartz. A computer controlled potentiostat (eDaq 401) is employed to control the external bias and to record the photocurrent generated. Full spectrum illumination was provided with a 15 W black light lamp (BLB Cosco SNI:04-6504-2001). The samples are anodically polarized at a scan rate of 25 mV/s under illumination, and the photocurrent is recorded. The photocurrent density versus potential (*j-V*) and photocurrent density versus time (*j-t*) curves of working electrode was carried out by the linier sweep voltametry (LSV) and multy pulsed amperometry (MVA) methods respectively.

Result and Discussion

Anodization Process and Morphology of Titanium Nanotubes

The process of synthesis of titanium nanotubes using electrochemical anodization method can be monitored by measuring the current generated at the electrode. Figure. 1, shows the current density-time curve recorded by a multimeter during electrochemical anodization of titanium foil in the ethylene glycol electrolytes. As can be seen clearly, similar trend is evident for electrochemical anodization under different potentials, which is the typical behavior titanium anodization process. At the initial stage of the anodization, the current density decrease rapidly to a minimum value, which is due to the formation of a oxide layer on the surface of titanium foil (Eq.1). The oxide layer acts as a barrier layer, which is electronically less conductive than the titanium substrate. Therefore, it can increase the resistance and reduce the current significantly.   At the next stage, the current density increase, which is due to the formation of small pits and pores on the surface of oxide layer through chemical dissolution reaction (Eq.2).

$$Ti \ + \ 2H_2O \quad \rightarrow \quad TiO_2 \ + \ 4H^+ \ + \ 4e^- \hspace{4cm} (1)$$
$$TiO_2 \ 6F^- \ + \ 4H^+ \quad \rightarrow \quad TiF_6^{2-} \ + \ 2H_2O \hspace{4cm} (2)$$

When the rate of electrochemical oxidation of titanium and chemical dissolution of TiO$_2$ reaches a dynamic equilibrium, the current gradually approaches to a steady state value. It is observable that the current density increases with increasing anodization voltage due to the enhancement of electric field intensity. The higher anodizing potential increases the driving force for ionic transport from the barrier layer (Ti/TiO$_2$ interface) into Ti metal, so that this process is expected to increase the diameter and length of the tube[32].
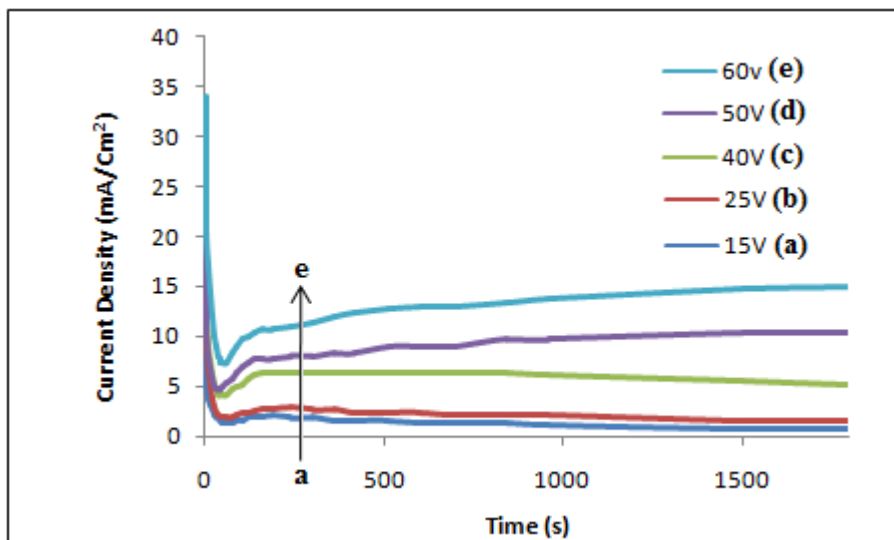
Figure.1. Current density-time curve for TiO$_2$ formation process under different anodization potentials

The top surface morphologies of TNTAs samples anodized under different potentials of 15 V, 25 V, 40 V, 50 V and 60 V are shown in Figure. 2(a)-(e), while the bottom surface morphology at 60 V is shown in Figure. 2(f). At 15 V of anodization potential, a homogeneous nanopores layer is observed clearly, which can be explained that the anodization voltage of 15 V is not high enough to reach the formation of TiO$_2$ nanotubes arrays in the ethylene glycol electrolyte. According to Eq. (2), fluoride ion plays a key role in the formation of TNTAs, which controls the chemical dissolution rate of TiO$_2$ layer. As we know, organic electrolytes base with high viscous severely restrict the diffusion of fluoride ion. Hence the formation of TNTAs needs a higher electric field in ethylene glycol electrolyte. At 25 V and 40 V anodization potentials, a mixed structure with a top nanoporous layer and an underneath highly ordered nanotube layer is appeared. The mixed structure is attributed to the fact that the thin nanoporous layer on the top surface of TiO$_2$ is not completely dissolved during the anodization process for 30 min in this experiment. At 50 V and 60 V anodization potentials, a homogeneous tubular structure is observed on the top layer and on the underneath layer. Figure. 2(f), we can see that the TiO$_2$ nanotube arrays anodized at 60 V exhibit hexagonal packing mode at the bottom and are still highly ordered and compacted which each other at the top.These anodization potentials are high enough to reach the formation of TNTAs in the ethylene glycol electrolyte.

Furthermore, it is found that the average inner diameter of TNTAs increase with increasing anodization potential. As anodization voltage increases from 15 V to 60 V, the pore diameter ranges from 15 nm to 90 nm. The effect anodization potential on the average pore diameter of TiO$_2$ samples is summarized in Figure. 3. Obliviously the pore diameter depend linierly on the anodization potentials,which consistent with other previous reports[32-33]. Based on the TNTAs growth mechanism, anodization process is competition of electrochemical oxidation (Eq. 1) and chemical dissolution (Eq. 2). As the barrier layer formed at the initial anodization, small pits originate in this oxide layer due to the localized dissolution of the oxide. Then the increase in electric field intensity improves electrochemical etching rate, resulting in further pore growth. The deeper pores grow, the higher the electric field intensity is required in these metallic regions, which enhances field-assisted oxide growth and chemical dissolution of the oxide. Therefore, well-defined interpore voids begin forming. After this, both the voids and tubes grow in equilibrium to form the final tubular structure. Thus improving anodization potential could promote the growth of pores and nanotube layers simultaneously.
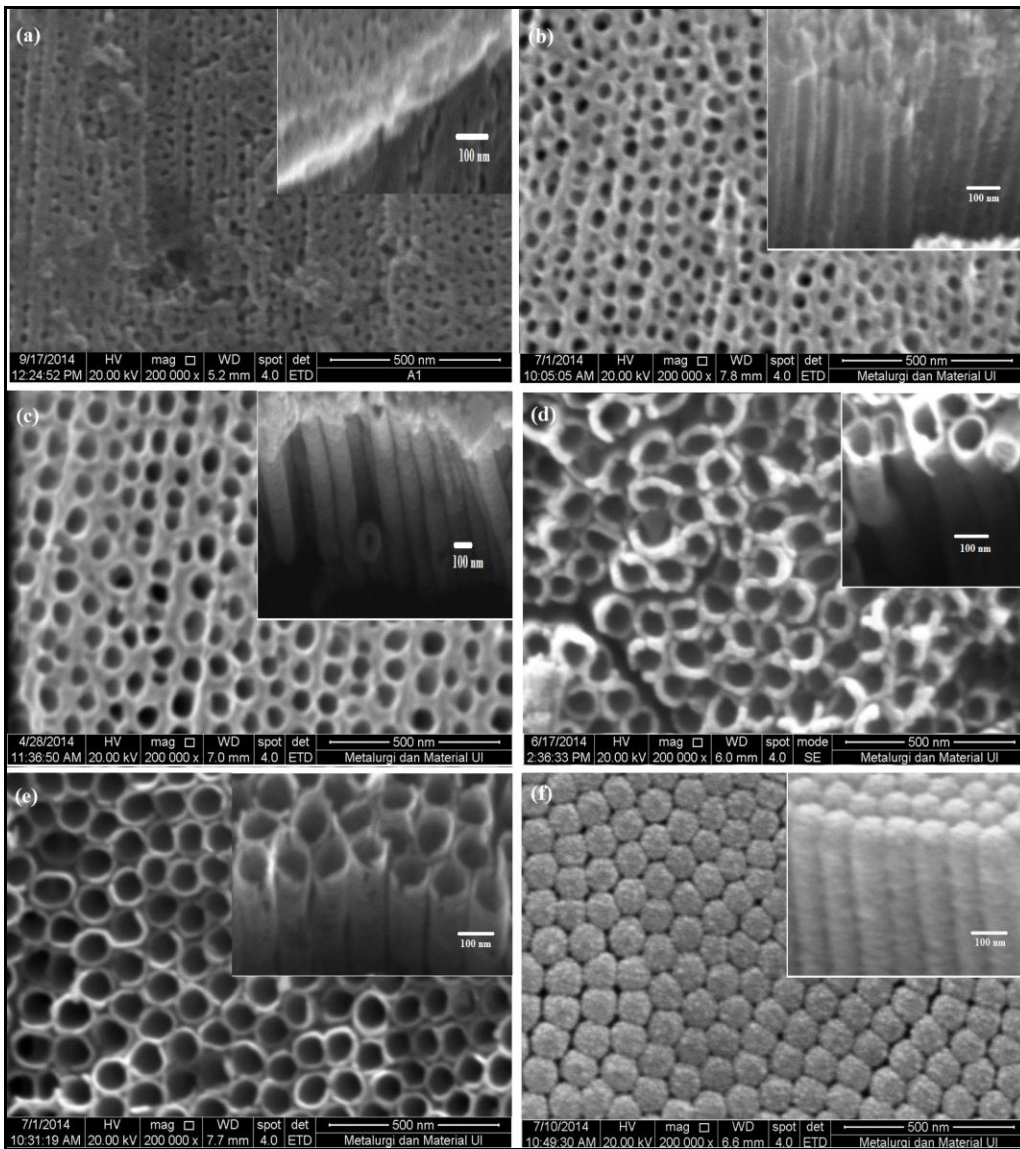
Figure. 2. FESEM image of top surface TiO$_2$ nanotubes arrays anodized under various potentials: (a) 15, (b) 25, (c) 40, (d) 50, (e) 60V and (f)bottom surface view of 60V, with inset image are cross section views.
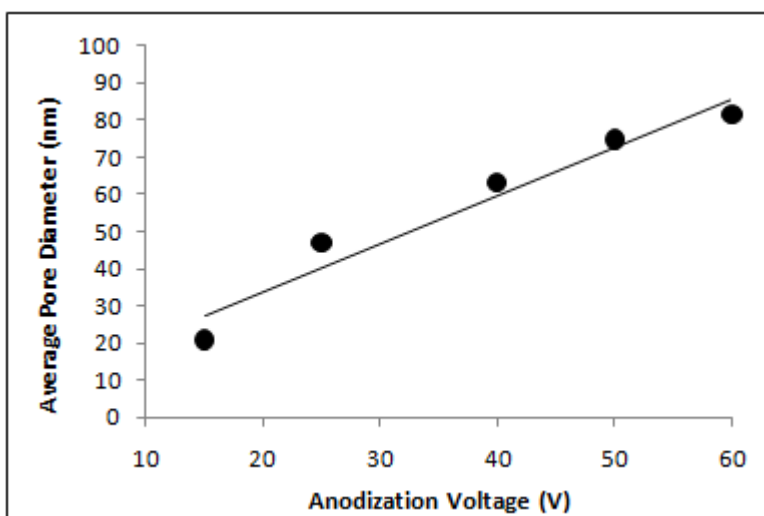

Figure 3. Effect anodization potentials on the average pore diameter of TiO$_2$ Nanotube

Photocurrent Response

The transient photocurrent response of TiO_2 nanotubes was measured in the one-compartment PEC cell under light illumination at zero bias. As shown in Figure. 4(a), the current value is approximately 0 mA/cm^2 in dark condition while the photocurrent rapidly rises to a constant value upon illumination. All photocurrent patterns of TiO_2 samples anodized under different potentials are highly reproducible for several light on-off cycles. This result indicates that TiO_2 nanotubes prepared in this study exhibit good photo response and fast charge transfer.

The average photocurrent measured during the 3 light on-off cycles as a function of anodized potentials is shown in Figure. 4(b). The result that the photocurrent increase linearly with increasing anodization potential. It is well-known that increasing the anodization potential can increase the pore diameter and the tube length, and it could provide a larger active surface area and higher absorption of incident photons, which leads to more photo generated electron-hole pairs[34-35]. Anodizing process with high potential also produces a dense tubular structure and uniform, so as to enhance the electron transfer process is characterized by an increased value of the photocurrent in a photoelectrochemical system. In the photoelectrochemical system, a higher photocurrent would correspond to a higher efficiency of the PEC device for solar hydrogen generation via water splitting process, as the current is related to the electron needed to reduce the H^+ ions into H_2 at the Pt cathode.
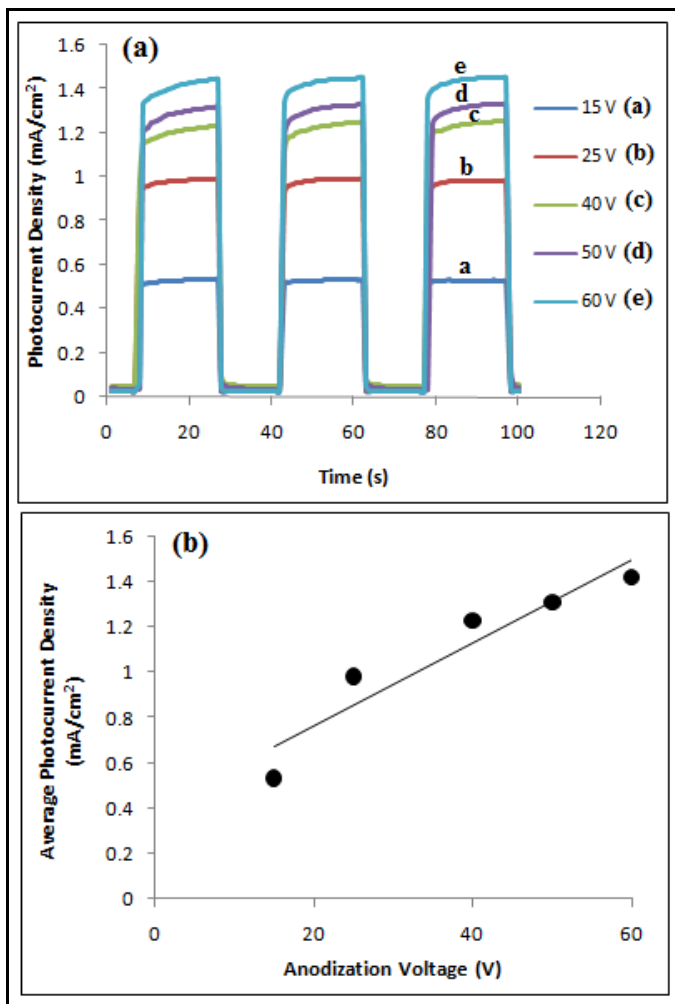

Figure. 4. The photocurrent response of TiO_2 nanotubes anodized (a) and the average photocurrent (b) as function of anodization potentials

Further study of photoelectrochemical behavior of TNTAs anodized under various potentials was determined by linier sweep voltametry at a scan rate 25 mV/s from -1.3 V to 1.0 V (vs Ag/AgCl). As all the dark currents of TNTAs samples are very small (around 10^{-3} mA/cm^2) and the dark I-V curves are superposed practically, Figure.5(a) only shows the dark current of TNTAs anodized at 25 V. However, with the

illumination, the photocurrent density increases with the increase of applied potential and gradually reaches a plateau value, which demonstrates typical behavior of n-type semiconductor. The result clearly shows that the anodization potential significantly affect the photoelectrochemical performance of TNTAs. The photocurrent increases with increasing anodization potential and the maximum photocurrent is obtained of TNTAs anodized at 60 V. The open circuit potential (OCP) and steady state potential (SSP) of TNTAs decrease with increasing anodization potential. At 15 V and 60 V anodization voltages, the OCP value are -0.73 V and -0,91 V, while the SSP value are -0.166 V and -0.470 V. The charge separation and accumulation of electrons in the semiconductor-electrolyte interface would be better on a smaller potential. The enhancement of the charge separation, translating into an improvement of the photocurrent response.

For determine of water splitting photo conversion efficiency of TiO_2 nanotube arrays electrode could be calculated by the following equation[36]:

$$\eta(\%)=j_p[(E^0_{rev} - E_{app})/I_0]x100 \qquad\qquad (3)$$

where j_p is the photocurrent density (mA/cm^2), $j_pE^0_{rev}$ is the total power output, j_pE_{app} is the electrical power input, and I_0 is the power density of incident light. E^0_{rev} is the standard reversible potential of 1.23 V/NHE and the applied potential is $E_{app}=E_{meas} - E_{aoc}$, where E_{meas} is the electrode potential (vs Ag/AgCl) of the same working electrode under open circuit condition in the same electrolyte. As expected in Figure. 5(b), TNTAs anodized at 60V for 30 min exhibit a maximum photoconversion efficiency of 9.92% at -0.47 V vs Ag/AgCl. Moreover, a linier relationship between the maximum photoconversion efficiency of TNTAs samples and anodization potential is obtained in Figure. 5(c).
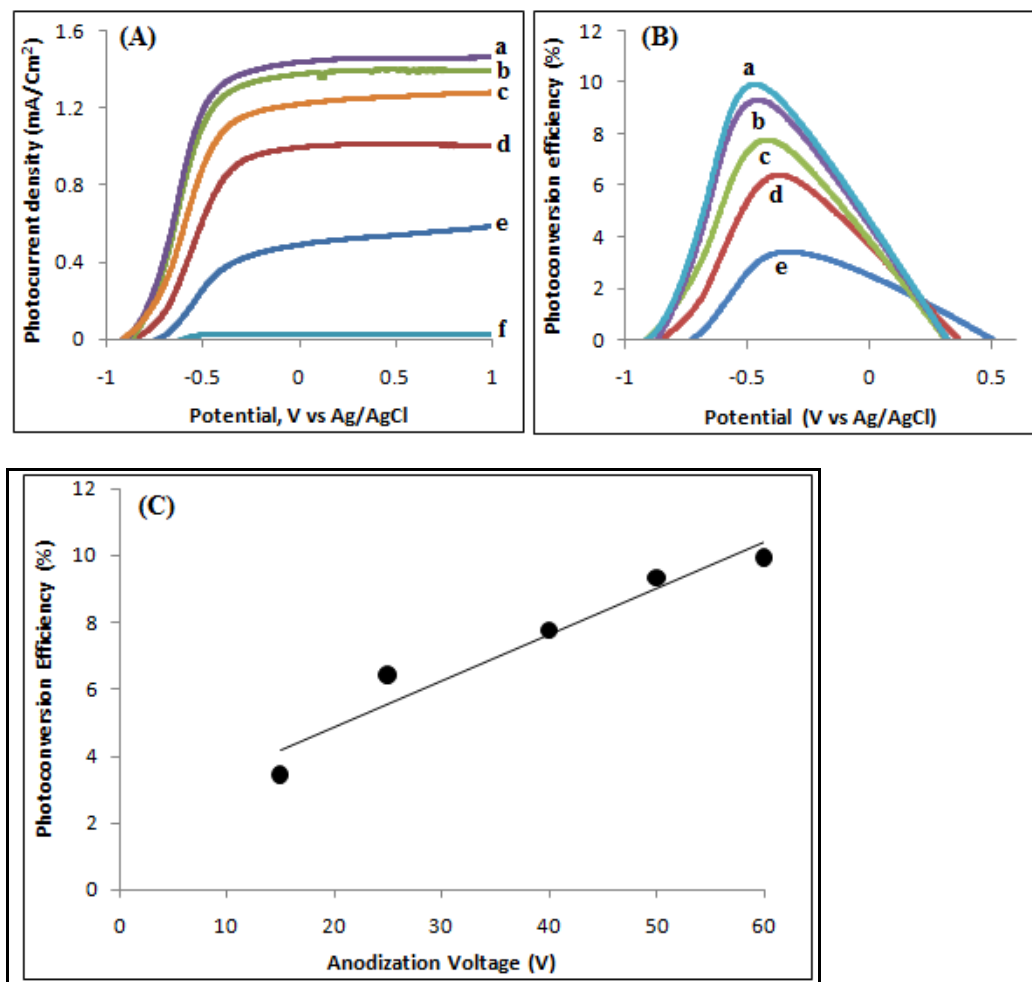

Figure.5. Photelectrochemical properties of TiO_2 nanotubes with various anodization potentials: (A) the-I-V curves, (B) corresponding photoconversion efficiency and (C) photoconversion efficiency as a function of anodization potential. (a) 60V, (b) 50V, (c) 40V, (d) 25V, (e) 15V and (f) 25V for dark condition.

Conclusion

The highly ordered nanotube arrays has been prepared by anodic oxidation of titanium foil under different anodization potentials in ethylene glycol electrolytes containing NH_4F and water. By varying anodization from 15 V to 60 V, the pore diameter increase from 15 to 80 nm. The photocurrent increase with increasing anodization potential, while anodizing process at 60 V; 30 minutes produces a dense tubular structure and uniform, so as to enhance the electron transfer process that is attributed by an increased value of the the overall solar-to-hydrogen efficiency of the photoelectrohemical water slitting.

Acknowledgment

References

1. Wang C, Hu Q, Huang J, Wu Lan, Deng Z, Liu Z, Liu Y, and Cao Y. Efficient hydrogen production by photocatalytic water splitting using N-doped TiO_2 film, J. App.Surf.Science., 2013, 283:188-192.
2. Li Y, Yu H, Zhang C, Song W, Li G, Shao Z, and Yi B. Effect of water and annealing temperature of anodized TiO_2 nanotubes on hydrogen production in photoelectrochemical cell, Electrochem.Acta., 2013,107:313-319.
3. Kamat P.V. Quantum Dot Solar Cells. The Next Big Thing in Photovoltaics, J.Phys.Chem.Lett., 2013,4:908-918.
4. Nojik J, Beard M.C, Luther J.M, Law M, Ellingson R.J, and Johnson J.C. Semiconductor Quantum Dots and Quantum Dot Arrays and Applications of Multiple Exciton Generation to Third-Generation Photovoltaic Solar Cells. Chem.Rev., 2010, 110:6873-6890.
5. Realpe A, Nunes D.P, Herrera A. Synthesis of Fe-TiO_2 Nanoparticles for Photoelectrochemical Generation of Hydrogen. Int.J. ChemTech.Res.,2016, 9:453-464.
6. Xu Q.C, Wellia D.V, Ng Y.H, Amal R, and Tan T. Synthesis of Porous and Visible-Light Absorbing Bi2WO$_6$ /TiO_2 Heterojunction Films with Improved Photoelectrochemical and Photocatalytic Performances, J.Phys.Chem.C., 2011, 115: 7419-7428.
7. Kang Q, Cai Q, Yao S.Z, Grimes C.A, and Ye Z. Fabrication of ZnxCd1−xSe Nanocrystal-Sensitized TiO_2 Nanotube Arrays and Their Photoelectrochemical Properties, J.Phys.Chem.C., 2012, 116:16885-16892.
8. Kum J.M, Yoo S.H, Ali G, and Cho S.O. Photocatalytic hydrogen production over CuO and TiO_2 nanoparticles mixture, Int.J.Hydrogen.Energy., 2013, 38:13541-13546.
9. Supriyono, Krisnandi Y.K, Gunlazuardi J. Band Gap Energy Modification of TiO_2 Photoelectrode by PbS/CdS Quantum Dots to Enhance Visible Region Photocurrent, Int.J. ChemTech Res., 2016, 9:191-198.
10. Mills A and Le Hunte S. An Overview of Semiconductor Photocatalysis, J.Photochem.Photobiol A:Chemistry., 1997, 108:1-35.
11. Linsebigler A.L, Lu G, and Yates J.T. Photocatalysis on TiO_2 Surfaces: Principles, Mechanisms, and Selected Results, Chem.Rev., 1995, 95:735-758.
12. Zhou Q, Fang Z, Li J and Wang M. Applications of TiO_2 nanotube arrays in environmental and energy fields: A review, Micropor.Mesopor.Materials., 2015, 202: 22-35.
13. Abdulrazzak F.H, Enhance Photocatalytic Activity of TiO_2 by Carbon Nanotube, Int.J. ChemTech.Res., 2016:9: 431-443.
14. Lei B.X, Lou Q.P, Sun, Z.F, Kuang D.B, and Su C.Y. Fabrication of partially crystalline TiO_2 nanotube arrays using 1, 2-propanediol electrolytes and application in dye-sensitized solar cells, Adv. Powd.Tech., 2013, 24:175-182.
15. Albu S.P and Schmuki P. Influence of anodization parameters on the expansion factor of TiO_2 nanotubes, Electrochem.Acta., 2013, 91:90-95.
16. HarshaVarthan S, Saravanakannan V, Chandiramouli R. Optimazion of Tubelength in TiO_2 Nanotube a Computational Approce, Int.J. ChemTech Res., 2015, 8:140-145.

17. Balasundaram T, and Raja K. Study of Well Structured Titanium Nanotube Anode Synthesis for Solar Cell Application by Electrochemical Anodization Method, Int.J.ChemTech Res.,2014,7:113-118.
18. Yuan Z.Y and Su B.L., Titanium oxide nanotubes, nanofibers and nanowires, Colloidd and Surface A:Physicochem.Eng.Aspects., 2004, 241:14
19. Wang Q, Hu G.Q, Duan X.F, Sun H.L and Xue Q.K. Microstructure and formation mechanism of titanium dioxide nanotubes, Chem.Phys.Lett., 2002, 365:427-431.
20. Michailowski A, Al Mawlawi D, Cheng G and Moskovits M. Highly Reguler Anatase Nanotubule arrays Fabricated in Porous anodic Template, Chem.Phis.Lett., 2001, 349: 1-5.
21. Kasuga T, Hiramatsu M, Hoson A, Sekino T, and Niihara K.,Formation of Titanium Oxide Nanotube, Langmuir., 1998, 14:3160-3163.
22. Mor K.G, Shankar K, Paulose M, Varghese O.K and Grimes C.A. Enhanced Photocleavage of Water Using Titania Nanotube Arrays, Nano.Lett., 2005, 5:191-195.
23. Paulose M, Shankar K., Yoriya S, Prakasam H.E, Varghese O.K, Mor G.P, Latempa T.A, Fitzgerald A and Grimes C.A. Anodic Growth of Highly Ordered TiO_2 Nanotube Arrays to 134 µm in Length, J.Phys.Chem.B., 2006, 110:16179-16184.
24. Prakasam H.E, Shankar K, Paulose M, Varghese O.K and Grimes C.A. A new Benchmark for TiO_2 Nanotube Array Growth by Anodization, J. Phys. Chem.C., 2007, 111:7235-7241.
25. Regonini D, Bowen C.R, Jaroenworaluck A and Stevens R. A review of growth mechanism, structure and crystallinity of anodized TiO_2 nanotubes, Mater.Scien.Engin., 2013, 74:377-406.
26. Lee K, Mazare A and Schmuki P. One-Dimensional Titanium Dioxide Nanomaterials: Nanotubes, Chem.Rev., 2014, 114:9385-9454.
27. Macak J.M, Tsuchiya H, Ghicov A, Yasuda K, Hahn R, Bauer S and Schnuki P. TiO_2 nanotubes: Self-organized electrochemical formation, properties and applications, Current opinion in Solid state and Materials Science., 2007, 11:3-18.
28. Mazare A, Paramasiyam I, Steina F.S, Lee K, Demetrescu I and Schmuki P. Flame annealing effects on self-organized TiO_2 nanotubes, Electrochem.Acta., 2012, 66:12-21.
29. Ni J, Noh K, Frandsen C.J, Kong S.D, He G, Tang T and Jin S. Preparation of near micrometer-sized TiO_2 nanotube arrays by high voltage anodization, Mater.Scien.Engin.C., 2013, 33:259-264.
30. Omidvar H, Goodarzi S, Seif A and Azadmehr A.R. Influence of anodization parameters on the morphology of TiO_2 nanotube arrays, Superlattices and Microstructures., 2011, 50:26-39.
31. Regonini D, Jaroenworaluck A, Stevens R and Bowen C.R. Effect of Heat Treatment on The Properties and Structure of TiO_2 Nanotubes: Phase Composition and Chemical Composition, Surface and Interface Analysis., 2010,42:139-144
32. Liang S, He Jingfu, Sun Z, Liu Q, Jiang Y, Cheng H, He Bo, Xie Z and Wei S. Improving Photoelectrochemical Water Splitting Activity of TiO_2 Nanotube Arrays by Tuning Geometrical Parameters, J. Phys.Chem.C., 2012, 116:9049-9053.
33. Sun Y and Yan, K.P. Effect of anodization voltage on performance of TiO_2 nanotube arrays for hydrogen generation in a two-compartment photoelectrochemical cell. Int.J.Hydrogen.Energy., 2014, 39: 11368-11375.
34. Kim T.H, Lee J.W, Kim B.S, Cha H and Nah Y.C. Morphological investigation of anodized TiO_2 nanotubes fabricated using different voltage conditions. Micropor.Mesopor.Materials., 2014, 196:41-45.
35. Adan C, Marugan J, Sanchez E, Pablos C, Grieken R.V. Understanding the effect of morphology on the photocatalytic activity of TiO_2 nanotube array electrodes. Electrochem.Acta., 2016, 191:521-529.
36. Sun Y, Wang G, Yan K. TiO_2 nanotubes for hydrogen by photocatalytic water splitting in a two-compartment photoelectrochemical cell. Int.J.Hydrogen.Energy., 2011, 36:15502-15508.

✶✶✶✶✶